Journal of Inflammation Research

Dovepress
open access to scientific and medical research

Open Access Full Text Article

ORIGINAL RESEARCH

Mesenchymal Stem Cells Ameliorate DSS-Induced Experimental Colitis by Modulating the Gut Microbiota and MUC-1 Pathway

Han Wang[1,2,*], Yang Sun[1,2,*], Feng-Jun Xiao[3,*], Xia Zhao[2,4], Wei-Yuan Zhang[1,2], Yu-Jun Xia[1], Li-Sheng Wang[1,2]

[1]School of Basic Medicine, Qingdao University, Qingdao, 266071, People's Republic of China; [2]Laboratory of Molecular Diagnosis and Regenerative Medicine, The Affiliated Hospital of Qingdao University, Qingdao, 266000, People's Republic of China; [3]Beijing Institute of Radiation Medicine, Beijing, 100850, People's Republic of China; [4]Department of Hematology, The Affiliated Hospital of Qingdao University, Qingdao, 266000, People's Republic of China

*These authors contributed equally to this work

Correspondence: Li-Sheng Wang, Laboratory of Molecular Diagnosis and Regenerative Medicine, The Affiliated Hospital of Qingdao University, Qingdao, 266000, People's Republic of China, Email lishengwang@qdu.edu.cn; Yu-Jun Xia, School of Basic Medicine, Qingdao University, Qingdao, 266071, People's Republic of China, Email xiayujun62@163.com

Journal of Inflammation Research downloaded from https://www.dovepress.com/
For personal use only.

Purpose: Mesenchymal stem cells (MSCs) have become novel therapeutic agents for the treatment of inflammatory bowel diseases (IBDs). However, the precise cellular and molecular mechanisms by which MSCs restore intestinal tissue homeostasis and repair the epithelial barrier have not been well elucidated. This study aimed to investigate the therapeutic effects and possible mechanisms of human MSCs in the treatment of experimental colitis.

Methods: We performed an integrative transcriptomic, proteomic, untargeted metabolomics, and gut microbiota analyses in a dextran sulfate sodium (DSS)-induced IBD mouse model. The cell viability of IEC-6 cells was determined by Cell Counting Kit-8 (CCK-8) assay. The expression of *MUC-1* and ferroptosis-related genes were determined by immunohistochemical staining, Western blot, and real-time quantitative polymerase chain reaction (RT-qPCR).

Results: Mice treated with MSCs showed notable amelioration in the severity of DSS-induced colitis, which was associated with reduced levels of proinflammatory cytokines and restoration of the lymphocyte subpopulation balance. Treatment with MSC restored the gut microbiota and altered their metabolites in DSS-induced IBD mice. The 16s rDNA sequencing showed that treatment with MSC modulated the composition of probiotics, including the upregulation of the contents of *Firmicutes, Lactobacillus, Blautia, Clostridia, and Helicobacter* bacteria in mouse colons. Protein proteomics and transcriptome analyses revealed that pathways related to cell immune responses, including inflammatory cytokines, were suppressed in the MSC group. The ferroptosis-related gene, *MUC-1*, was significantly upregulated in the MSC-treated group. *MUC-1*-inhibition experiments indicated that *MUC-1* was essential for epithelial cell growth. Through overexpression of *MUC-1*, it showed that upregulation of *SLC7A11* and *GPX4*, and downregulation of *ACSL4* in erastin and RSL3-treated IEC-6 cells, respectively.

Conclusion: This study described a mechanism by which treatment with MSCs ameliorated the severity of DSS-induced colitis by modulating the gut microbiota, immune response, and the *MUC-1* pathway.

Keywords: inflammatory bowel disease, mesenchymal stem cells, gut microbiota, MUC-1, multi-omics

Introduction

Mesenchymal stem cells (MSCs) have been approved as novel therapeutic agents for the treatment of inflammatory bowel diseases (IBDs) in clinical trials, including ulcerative colitis and Crohn's disease.[1] MSCs, which are well-known immunomodulatory agents, are effective agents for promoting tissue repair and regeneration.[2] Systemic administration of MSCs derived from various resources, such as bone marrow, adipose tissues, and umbilical cord (UC), shows beneficial effects in the treatment of IBD. Allogenic adipose-derived MSCs, which have long-term efficacy and safety for use in complex perianal fistulas in patients with Crohn's disease, have been approved in Europe.[3] Moreover, MSCs derived

Received: 16 January 2023
Accepted: 27 April 2023
Published: 11 May 2023

© 2023 Wang et al. This work is published and licensed by Dove Medical Press Limited. The full terms of this license are available at https://www.dovepress.com/terms.php and incorporate the Creative Commons Attribution – Non Commercial (unported, v3.0) License (http://creativecommons.org/licenses/by-nc/3.0/). By accessing the work you hereby accept the Terms. Non-commercial uses of the work are permitted without any further permission from Dove Medical Press Limited, provided the work is properly attributed. For permission for commercial use of this work, please see paragraphs 4.2 and 5 of our Terms (https://www.dovepress.com/terms.php).

from umbilical cord and bone marrow have been investigated in clinical trials for treatment of IBD.[4,5] Preclinical and clinical studies have validated the benefits of MSC treatment for IBD by maintaining intestinal integrity and tissue repair.[1,6] The clinical outcomes of MSCs derived from various resources will be investigated in further clinical trials.

Treatment with MSC ameliorates colitis inflammation by repairing the intestinal epithelial barrier injury and regulating immune responses. Regulation of the anti-inflammatory pathways and cytokine levels are considered a major mechanism underlying the effects of MSC on IBD.[1,7] Human umbilical cord-derived MSCs (UC-MSCs) alleviate IBD by inhibiting neutrophils infiltration in intestinal tissues.[8] Moreover, extensive studies have revealed that MSCs secrete growth factors and release activated exosomes. MSC-derived exosomes also act as effectors in repairing the mucosal barrier and restoring intestinal immune homeostasis in mouse IBD models.[9] Multiple studies have shown that MSC-derived exosomes attenuate colitis via miRNA-mediated regulation of macrophage pyroptosis.[10] MSCs promoted epithelial cell proliferation to accelerate mucosal healing in a murine colitis model via TSG-6 mediated pathways.[9] Furthermore, MSC-mediated regulation of T-regulatory cells and macrophages is also involved in IBD.[11]

One of the therapeutic effects of MSCs on IBD includes the healing of epithelial barriers. MSCs promote the regeneration and integrity of the colon epithelial tissue by upregulating the level of circulating insulin-like growth factor 1 (IGF-1) in mice with colitis.[12] Moreover, treatment with MSCs significantly increases intestinal epithelial cell proliferation, intestinal stem cell regeneration and intestinal angiogenesis.[13] MSCs-exosomes treatment protected mice against IBD by restoring mucosal barrier repair and intestinal immune homeostasis via TSG-6 pathway.[9] However, the precise mechanisms by which MSCs promote intestinal barrier regeneration in IBD require further investigation. Advanced studies of the gut microbiota and their metabolites indicated that they may be involved in the mechanism underlying the therapeutic effect of MSCs in IBD. Moreover, emerging modalities elucidated the treatment with UC-MSCs influence the gut microbiota composition, including increased microbial diversity, and alters the abundance of metabolites.[14] MSC-derived exosomal miRNAs can alleviate experimental colitis by promoting intestinal barrier function and affecting the gut microbiota.[14] In this context, this study aimed to investigate the therapeutic effects and possible mechanisms of human UC-MSCs in the treatment of experimental colitis in mice by performing an integrative analysis of the transcriptome, proteomics, metabolomics, and gut microbiota.

Methods

Reagents and Antibodies

Dextran sulfate sodium salt (DSS, MW 36000–50,000 Da, CAS: 9011–18-1) was obtained from MP Biomedicals (Solon, OH, USA). Anti-mouse antibodies (CD3 PE-Cy7; CD4 FITC; CD8 PE/PerCP; Ly6G V450; F4/80 FITC; Foxp3 PE) used for flow cytometry were purchased from BioLegend (San Diego, CA, USA).

MSCs

The MSC products are Good Manufacturing Practice (GMP) grade products and were kindly provided by the Platinumlife Biotechnology Co., Ltd (Beijing, China). The MSCs were separated from human umbilical cord and to prepare a single-cell suspension (1×10^6 cells/mL). MSCs were cultured in MSC basic medium (Clin-Biotech, Beijing, China). Cells were trypsinized into single cells using 0.05% trypsin (Procell, Wuhan, China) and passaged until reaching 80% confluence. Passage 5 cells were used in the experiments.

Animal Studies and Colitis Induction

Animal studies were performed according to the Guide for the Animal Care and Use of Laboratory Animals. The study was approved by the Animal Care and Use Committee of the Affiliated Hospital of Qingdao University (approval number AHQU-MAL20210930). Male C57BL/6 mice (6–8 weeks old) were housed under specific pathogen-free (SPF) conditions with free access to food and water. Three groups of mice were allocated for experiments: negative control (NC) group (n=5), DSS+ phosphate-buffered saline (PBS) group (n=10), DSS+MSC group (n=10). The number of experimental animals meets the statistical requirements and animal principles. Acute colitis was induced by giving mice drinking water containing 2.5% DSS for 7 days. GMP-Grade UC-MSCs (10^6 every mouse) resuspended with PBS were administered twice on days 3 and 5 to the mice through tail intravenous injection (Figure 1A). Figure 1A shows the schedule for UC-MSC administration in the DSS-induced

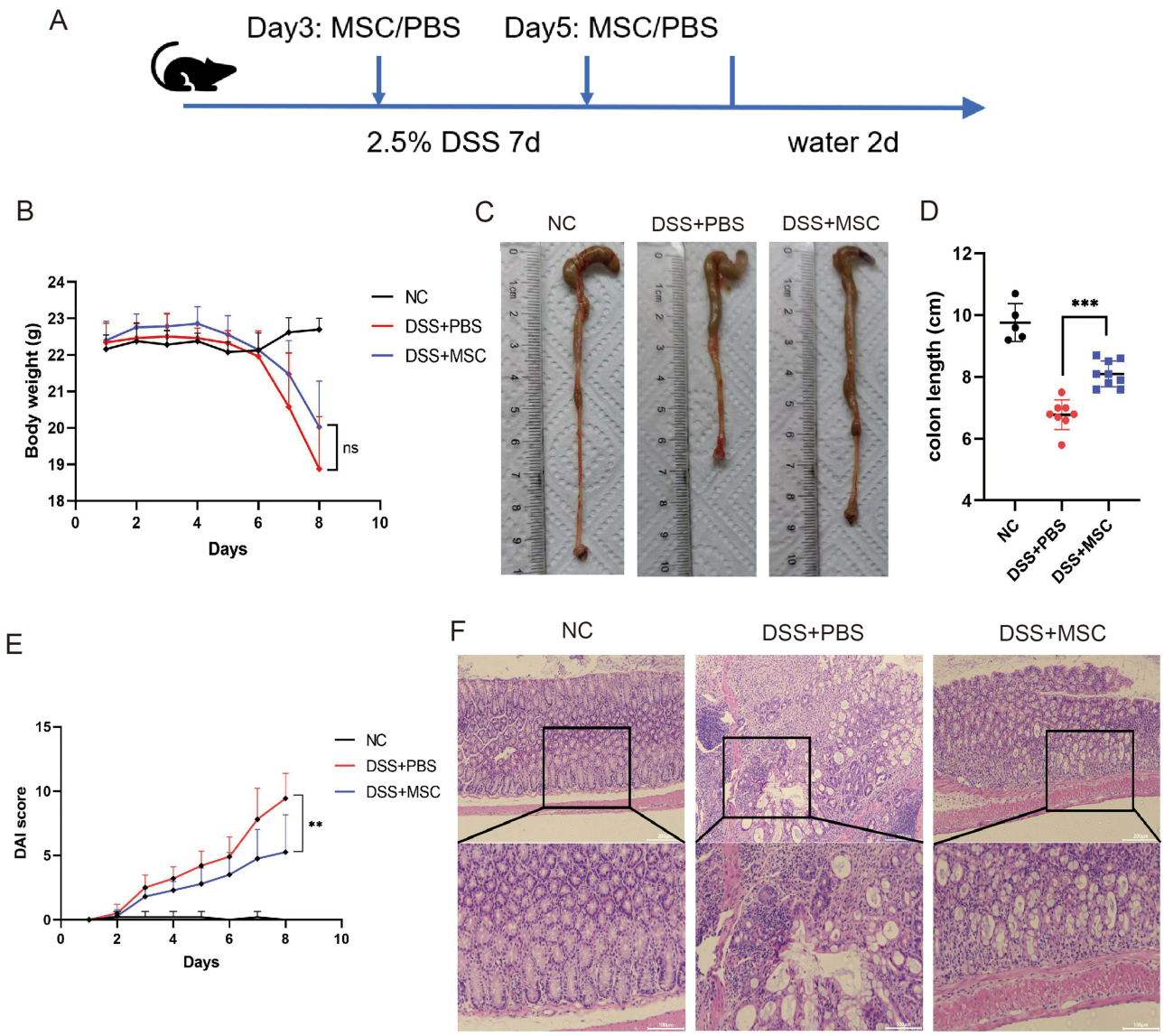

Figure 1 Treatment with MSC alleviates DSS-induced colitis model in mice. (**A**) The experimental process of DSS-induced acute colitis and treatment with MSC. The colitis was induced by 2.5% DSS dissolved in water for 7 consecutive days. Every mouse received a tail intravenous injection of 1×10^6 MSCs or PBS on days 3 and 5 (n=10). The negative control (NC) group mice were given untreated water (n=5). (**B**) The body weight of mice on each day. (**C**) Representative photographs of mice colons taken from every group. (**D**) The statistical graph of colon length from each group. (**E**) The Disease Activity Index (DAI) of each mouse group. (**F**) Hematoxylin and eosin staining of the colon tissue in each group (scale bar: 200 μm top graph/100 μm bottom graph). Data are presented as mean ± SD. ***P < 0.001, **P < 0. 01.
Abbreviation: ns, no significance.

colitis model. In the DSS+PBS group, colitis was induced similarly to the DSS+MSC group; however, instead of administering MSCs on days 3 and 5, same volume of PBS was administered through tail intravenous injection. The NC group consisted of mice given normal food and water and acted as the negative control. Mice body weight, fecal characteristics, and fecal occult blood tests were recorded daily during the colitis induction and recovery phases of the experiment. The Disease Activity Index (DAI) was calculated daily according to previous protocols.[15]

Cell Surface Staining and Flow Cytometry Analysis

At the endpoint of the experiment, mice were sacrificed, and peripheral blood and spleen tissue were collected from the mice. Red blood cells from the peripheral blood were lysed according to the manufacturer's instructions (BioLegend). Residual peripheral immune cells were then stained with flow cytometry antibodies for 30 min. Spleen tissues were ground and filtered to prepare a single-cell suspension, which was then washed with PBS, and stained with flow

cytometry antibodies. Flow cytometry analysis was performed on FACSCelesta™ (BD Biosciences, USA) and analyzed using FlowJo V10 software (TreeStar, Ashland, OR, USA).

Hematoxylin and Eosin Staining

Colon tissues were collected at the end of the study period and immediately fixed with 4% paraformaldehyde. Tissue samples were embedded in paraffin and stained with hematoxylin and eosin. The specimens were observed under an inverted microscope (Model DMIL, Leica, Wetzlar, Germany) and photographed.

Quantitative Real-Time PCR (qRT-PCR)

Total RNA was extracted from mouse colon tissue or cell lysates using TRIzol reagent (Invitrogen, Thermo Fisher Scientific, Waltham, MA, USA). The RNA concentration was measured at A260nm and A280nm using a microplate reader (Molecular Devices, San Jose, USA). One μg RNA used for reverse transcription was synthesized using a TransScript® One-step cDNA synthesis kit (Transgen, Beijing, China). The SYBR Green qPCR SuperMix kit (Transgen) was used for qRT-PCR. Cycle threshold (Ct) values were determined using the Applied Biosystems QuantStudio 5 RT-PCR system (Thermo Fisher Scientific). The total volume of qRT-PCRs was 20μL. Primers were designed and synthesized by Sangon Biotech Co., Ltd (Beijing, China). Ppib and Eef2 were used as the internal reference of IEC-6 cells and DSS-induced colitis tissue, respectively. All primer sequences for mouse colon tissues are listed in Table 1. The reactions were performed in triplicate, and relative mRNA expression was calculated using the $2^{-\Delta\Delta Ct}$ method.

16S Ribosomal DNA Amplicon Sequencing

Fecal contents (NC, DSS+PBS, and DSS+MSC groups) were collected under sterile condition and frozen in liquid nitrogen then stored at −80°C, and every group contained three biological replicates. 16S ribosomal DNA analysis was performed by Applied Protein Technology Co., Ltd (Shanghai, China). Total microbial DNA was extracted from fecal sample using SDS method. DNA concentration and purity were monitored on 1% agarose gels, and DNA was diluted to 1ng/μL using sterile water. Amplicon was generated by PCRs with specific primers, which includes 16S V3-V4: 341F-806R, 18S V9: 1380F-1510R. PCR products were preformed electrophoresis on 2% agarose gel for detection. Samples with bright main strip between 400 and 450 bp were chosen for further experiments. Sequencing libraries were generated using NEB Next®Ultra™DNA Library Prep Kit for Illumina (NEB, USA) and sequenced on an Illumina Miseq/HiSeq2500 platform and 250bp/300bp paired-end reads were generated. STAMP software was used to confirm differences in the abundances of individual taxonomy between the two groups. Linear discriminant analysis effect size (LEfSe) was used for the quantitative analysis of biomarkers within different groups.

RNA Sequencing

Colon samples (NC, DSS+PBS, and DSS+MSC groups) were frozen in liquid nitrogen and stored at −80°C, and three samples from each group were randomly selected for RNA sequencing. Total RNA was extracted from three groups of colon samples using TRIzol reagent (Invitrogen) according to the manufacturer's instructions. RNA integrity and concentration were

Table 1 The Primer Sequences Used in qRT-PCR

Target	Forward (5'-3')	Reverse (5'-3')
SLC7A11	GGCACCGTCATCGGATCAG	CTCCACAGGCAGACCAGAAAA
GPX4	GATGGAGCCCATTCCTGAACC	CCCTGTACTTATCCAGGCAGA
ACSL4	CTCACCATTATATTGCTGCCTGT	TCTCTTTGCCATAGCGTTTTTCT
MUC-1 (mouse)	GGCATTCGGGCTCCTTTCTT	TGGAGTGGTAGTCGATGCTAAG
MUC-1 (rat)	GGTGGCTTTGGTCATCGTCTATCTC	TAGCGTCCGTGAGTGTGGTAGG
MUC-1 (human)	CTTCCTGCTGCTGCTCCTCAC	TCTCTGGGTAGCCGAAGTCTCC
Eef2	TGTCAGTCATCGCCCATGTG	CATCCTTGCGAGTGTCAGTGA
Ppib	CTGTCGATTCCCTCACAGGT	AAAATCAGGCCTGTGGAATG

performed. A cDNA library was constructed following the manufacturer's instructions of NEBNext Ultra RNA LibraryPrep Kit for Illumina (E7530; New England Biolabs [NEB], Ipswich, MA, USA) and NEBNext Multiplex Oligos for Illumina (NEB, E7500). The cDNA libraries were loaded onto an Illumina HiSeq sequencing platform (conducted by Applied Protein Technology). Adapters and reads from the raw reads of each sample were trimmed to obtain clean reads. Gene expression levels were estimated using fragments per kilobase of exon per million mapped fragments (FPKM). Differential genes were based on $P_{adj}<0.05$, $\log_2$fold change (FC)>1 as the significance criterion.

Proteomics Analysis

Colon samples (NC, DSS+PBS, and DSS+MSC groups) were frozen in liquid nitrogen and stored at −80°C. Differential proteins were performed by 4D-Label-free quantitative proteomics (Applied Protein Technology Co., Ltd). Every group contained three biological replicates. The analytical process included protein extraction, trypsin digestion, and high pH reversed-phase peptide fractionation. The proteins were identified and quantified. Finally, all the protein data were analyzed using bioinformatics, which includes identification quantitative analysis, differential expression analysis, and functional analysis. Identified proteins were shown on histogram and Venn diagram. The differential proteins were analyzed by volcano plot and hierarchical cluster. Functional analysis includes gene ontology (GO) and Kyoto Encyclopedia of Genes and Genomes (KEGG) analysis. Differential expression analysis and functional analysis of proteins were performed between groups.

Untargeted Metabolomics of Colon Tissues

We selected the same mice used for RNA sequencing and proteomics for untargeted metabolomics analysis. For consistency, each sample was selected from the same part of the colon tissue. The selected tissues were frozen in liquid nitrogen and stored at −80°C. Tissues were cut on dry ice of about 80 mg and homogenized using the homogenizer. Homogenized solution was mixed well with 800 μL methanol/acetonitrile (1:1, v/v) for metabolite extraction. The mixture was centrifuged for 15 min (14,000 g, 4 °C). The supernatant was dried and re-dissolved in 100 μL acetonitrile/water (1:1, v/v) solvent. All samples were separated using an Agilent 1290 Infinity LC ultra-high performance liquid chromatography (UHPLC) system (Agilent Technologies, Santa Clara, CA, USA) from Shanghai Applied Protein Technology Co., Ltd. The first and second spectrograms were collected by TripleTOF 6600 mass spectrometer (AB SCIEX, Framingham, MA, USA). Finally, XCMS software was used to analyze the significant metabolites in each group and their structures.

Cell Counting Kit-8 (CCK-8) Assay

Rat intestinal epithelial cell line No. 6 (IEC-6 cells) (iCell-r016, iCellbioscience, Shanghai, China) were cultured in DMEM medium (Gibco), supplied with 10% foetal bovine serum (FBS, Gibco) and 0.1U/mL insulin (MedChemExpress, MCE, Monmouth Junction, NJ, USA) based on ATCC protocol. Cells were seeded in 96-well plates at a density of $1\times10^4/cm^2$. The MUC-1 gene inhibitor GO-203 (MCE) was added to IEC-6 cells with different concentrations (10, 5, and 2.5μM). Moreover, ferrostatin-1 (fer-1, MCE) was added was added at a concentration of 1 μM with 5μM GO-203 to determine whether it could improve the cell viability. Then, 10μL of a CCK-8 solution (YEASEN, Shanghai, China) was added to each well and incubated at 37°C in the dark for 2h. The optical density (OD) levels were measured by microplate reader at 450nm (Molecular Devices).

Lentivirus Transduction

The MUC-1 overexpression lentivirus was constructed by Genechem Co., Ltd (Shanghai, China). The transcript sequence of MUC-1 is NM-001018016. The sequence element of lentivirus structure is shown in Figure S1E. IEC-6 cells were seeded into T25 culture flask. When cells reached 20–30% confluence, lentivirus and infection-enhancing fluid (Genechem) were added to culture medium with lentivirus-multiply of infection (MOI) of 10. After lentivirus transfection for 48–72h, 2μg/mL puromycin (MedchenExpress) was added to culture medium in order to harvest stabilizing MUC-1-overexpressed cells.

Immunohistochemical Staining

Colon tissues were collected at endpoint and embedded in paraffin; then, colon tissues go through deparaffinating, antigen retrieval, and blocked with serum. After blocking, colon samples were incubated with anti-MUC-1 (Servicebio, Wuhan, Hubei, China) at 4°C overnight. The second day, colon tissues were incubated with horseradish peroxidase (HRP)-labeled secondary antibody at 37°C for 1h. Next, several steps were conducted, including SABC reaction, DAB chromogenic, and tissue dehydration. The staining morphology was photographed using microscope (Leica). The H-score of intensity was analyzed by Aipathwell software (Servicebio).

Western Blot Assay

IEC-6 cells were lysed by RIPA lysis buffer (Meilunbio, Dalian, Liaoning, China). SDS loading buffer was added to the sample and incubated at 100°C for 10 min. Sample proteins were electrophoretically separated by 30% SDS-PAGE gels (Servicebio) and transferred to a 0.45μm polyvinylidene difluoride (PVDF) membrane. The proteins were blocked with 5% skim milk in Tris-buffered saline. Then samples were incubated with primary anti-MUC-1 (Servicebio) and anti-β-actin (Abclonal, Wuhan, Hubei, China) at 4°C overnight. Next, the samples were incubated with HRP-labeled goat anti-rabbit IgG H&L (Servicebio). Sample bands were visualized using enhanced chemiluminescence (ECL) and analyzed with the ProteinSimple instrument (Bio-Techne, Minnesota, USA).

Statistical Analysis

Data are presented as the mean ± standard deviation (SD) of at least three independent experiments, unless otherwise stated. Statistical significance of differences was assessed using Student's *t*-test for two groups. Data were analyzed by GraphPad Prism V9.0 software (San Diego, CA, USA). P values <0.05 were considered statistically significant.

Results

Intravenous Injection of UC-MSCs Attenuates DSS-Induced Colitis in Mice

Figure 1A shows the schedule for UC-MSCs application in a DSS-induced colitis mouse model. The mice in the DSS-treated groups significantly lost body weight, whereas mice in the DSS-MSC group slightly maintained their body weight (Figure 1B). Treatment with MSC resulted in less shortening of the colons compared to treatment with PBS (Figure 1C and D). Colon staining revealed that the severity of the injury assessed using Disease Activity Index (DAI) was lower in the DSS+MSC group than in the DSS group. Moreover, the administration of MSCs significantly improved the pathological changes in DSS-induced IBD mice (Figure 1E and F). The Histopathology Activity Index (HAI) was obtained from hematoxylin and eosin staining (Figure S1A). Collectively, these results indicate that UC-MSCs effectively attenuated DSS-induced colitis in mice.

Treatment with MSCs Suppresses Inflammatory Responses in DSS-Induced Colitis in Mice

Marked activation of the immune response and uncontrolled production of inflammatory cytokines were detected in DSS-induced mice (Figure 2). To understand the anti-inflammatory effects of MSCs on DSS-induced colitis in mice, we measured the levels of proinflammatory cytokines and chemokines in the peripheral blood serum, and the percentage of immune cells in peripheral blood and spleen tissues. Treatment with MSC significantly decreased the levels of cytokines such as IL-1β, TNF-α, and IL-6 in DSS-induced mouse models (Figure 2A) and recovered the percentages of CD3, CD4/CD8, B220, and Ly6G in the peripheral blood as well the percentages of CD3, CD4/CD8, T-reg, Ly6G, and F4/80 in the spleen (Figure 2B). The representative gating strategy of flow cytometry analysis was shown in Figure S2, including peripheral blood immune cells analysis (Figure S2A) and spleen cell analysis (Figure S2B and C). Thus, these findings validated that MSCs suppress inflammation responses by affecting growth cytokines and lymphocytes.

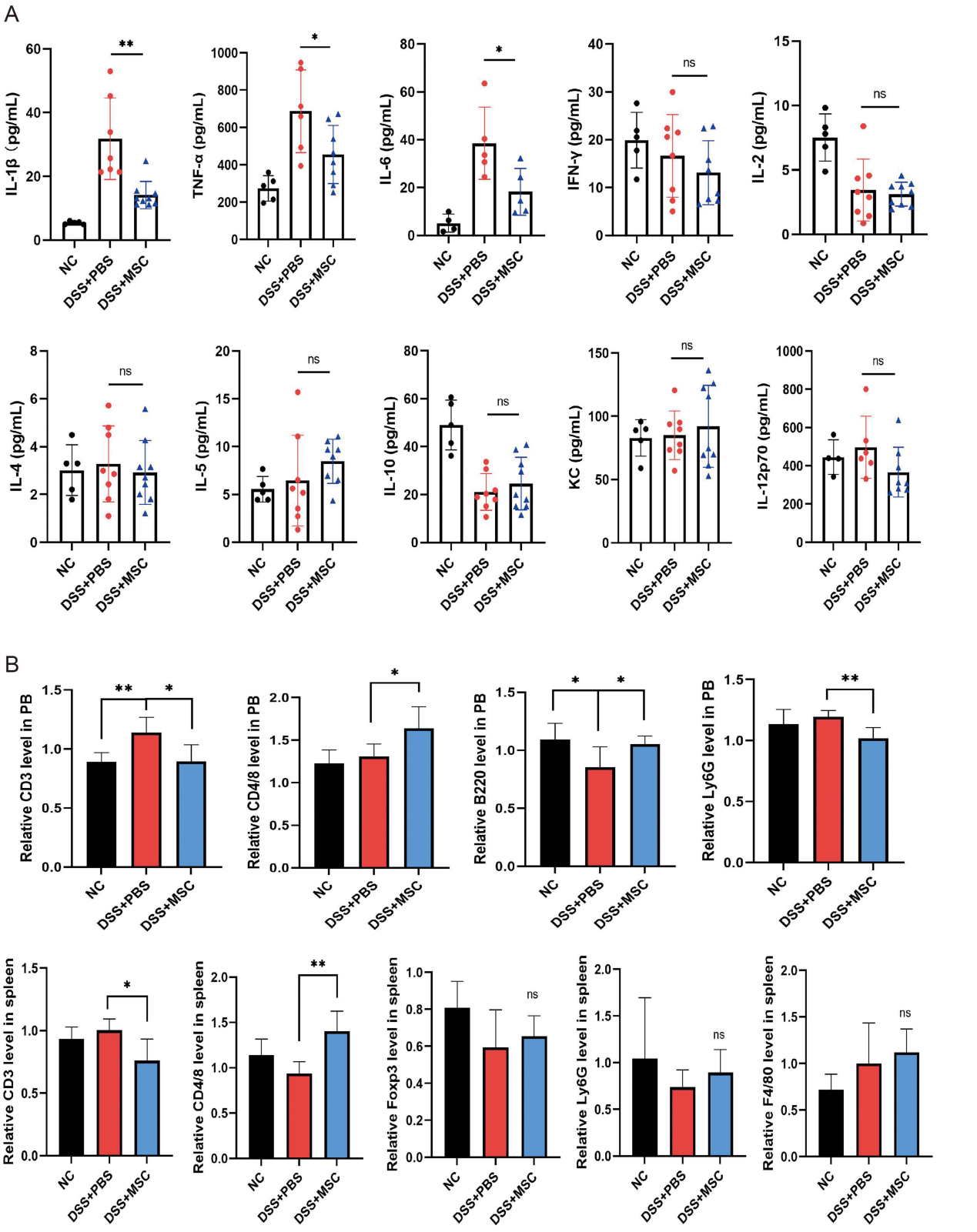

Figure 2 Treatment with MSCs suppresses the inflammatory response induced by DSS in mice. (**A**) The serum inflammatory cytokines were measured using Luminex 200 detection platform. (**B**) Immune cells in the peripheral blood and spleen detected by flow cytometry. Data are presented as mean ± SD. **P < 0.01, *P < 0.05.
Abbreviation: ns, no significance.

UC-MSCs Modify Gut Microbiota Composition and Increase the Microbial Flora

The gut microbiota plays an important role in the pathogenesis of experimental DSS-induced IBD models. Therefore, we performed high-throughput gene sequencing analysis of 16S rRNA in fecal bacterial DNA to determine the effect of MSCs on the gut microbiota composition. The diversity and characteristics of the colon microbiota were significantly altered in mice with DSS-induced colitis and those treated with MSC (Figure 3A and B). The cladogram of microbiota species was analyzed using the LEfSe, which indicated a statistically significant separation between the microbiota of DSS-PBS and DSS-MSC groups (Figure 3C, Figure S3A). The relative abundances of probiotics such as *Firmicutes, Blautia, Roseburia, Helicobacter*, and *Lactobacillus* in the microbiota, were significantly higher in the MSC-treated group than in the DSS-PBS group. The most significant function of 'replication and repair' and 'defense mechanisms' of the DSS-PBS (M) and DSS-MSC (T) groups was indicated by linear discriminant analysis (LDA) scores (Figure 3D and E). Changes in the gut microbiota were related to metabolic diseases and immune system (Figure 3F). Thus, treatment with UC-MSCs alters the gut microbiota composition and affects the immune system and tissue repair.

Changes in Colon Proteomics After Treatment with MSCs

We performed a proteomic analysis comparing the DSS-PBS and the DSS-MSC treatment groups to identify differentially expressed proteins between the two groups. We identified 41 upregulated proteins and 74 downregulated proteins (Figure 4A and B). Alg3, Txnip, and Tomm7 were significantly upregulated, whereas Naa16 and Sike1 were significantly downregulated in IBD models (Figure 4C). These proteins are associated with immune cells and cytokines.[16–19] The differential expression of the proteins can be observed in Figure S3B. GO classified annotation showed that the DSS-MSC treatment group was annotated to multiple terms within the three categories 'immune response', 'glucose import', and 'immune system process', suggesting a high abundance of various functional proteins in DSS-MSC-treated group (Figure 4D).

Untargeted Metabolomics Reveals That Ferroptosis and Glutathione Metabolism are Involved in the Effects of MSCs

A volcano plot of the differential metabolites showed significantly different metabolites in the positive/negative ion modes (OPLS-DA VIP>1, $P < 0.05$, MSC vs DSS group; Figure 5A and B). The hierarchical clustering heatmap of significantly different metabolites in the positive/negative ion mode is shown in Figure 5C. The upregulated metabolites included Gamma-glu-glu and Glu-Ser peptide in the positive ion modes and alpha-L-Glu-Gly and glutaric acid in the negative ion model. KEGG enrichment analysis revealed that the enriched metabolic pathways from the DSS-MSC group were related to ferroptosis and glutathione metabolism pathways (Figure 5D). The specific classes of metabolites to regulate ferroptosis have been implicated in the pathogenesis of IBD treated with MSCs.

Transcriptome Analysis Revealed That Treatment with MSCs Suppresses Immune Response Pathways

RNA-seq analysis was performed to obtain and compare the global transcriptomic profiles of the DSS-PBS and DSS-MSC groups. Differential gene expression analysis and the differential expressed genes (DEGs), including upregulated and downregulated genes, between the DSS-MSC and DSS-PBS groups, are shown in Figure 6A and B. Subsequently, we performed KEGG analysis to investigate the link between biological signaling pathways and the DEGs (Figure 6C). As shown in Figure 6D, GO enrichment analysis revealed that 'immune response', 'immune system process', and 'defense response' were the top three signaling pathways suppressed in the DSS-MSC group. Thus, the RNA-seq analysis confirmed that immune responses participate in the mechanism of MSCs in the treatment of IBD.

MUC-1 is Identified as an Epithelial Cell Regulator in the DSS-MSC Colitis Mouse Model

Based on the transcriptome profile of the DSS-MSC group, the expression of several target genes, such as *MUC-1* and *SLC7A11*, was validated in colon tissues (Figures 7A and S1B). What's more, the *MUC-1* protein level was further validated by immunohistochemistry assay. The DSS-MSC group showed higher expression level of *MUC-1* than the

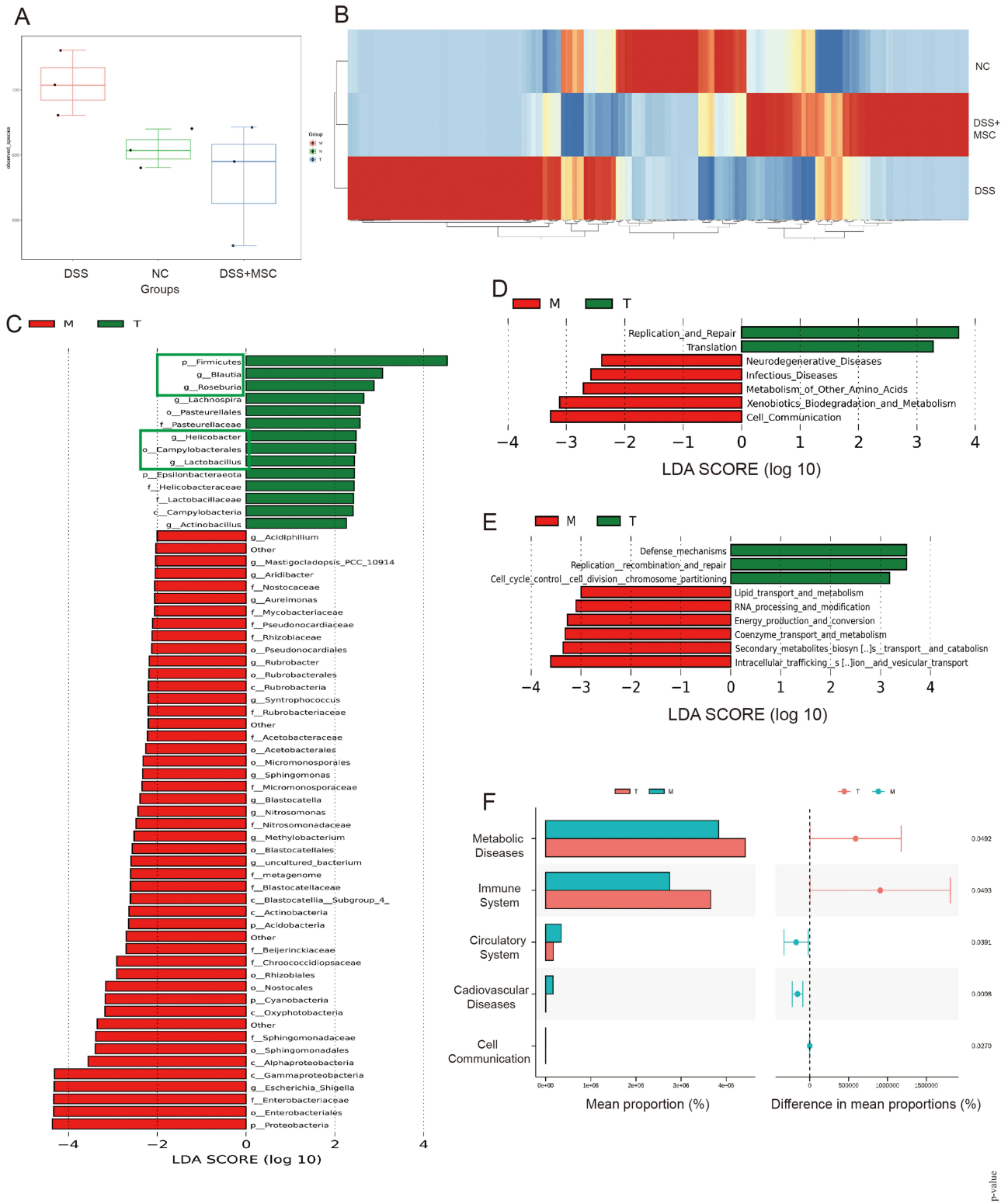

Figure 3 Treatment with MSCs significantly alters the diversity and features of the colon microbiota in DSS-induced colitis. (**A**) The diversity of gut microbiota in the three groups namely: the negative control (N), DSS (M) and DSS-MSC (T) groups. Tukey's tests were used to analyze the observed species index and the results are shown as standard boxplots. (**B**) Heatmap of genus species observed in NC, DSS and DSS-MSC group. (**C**) The LDA score of DSS (M) and DSS-MSC (T) group based on the taxonomy of LEfSe analysis. (**D**) The LefSe analysis results based on KEGG function prediction. The most significant function entries of DSS (M) and DSS-MSC (T) group were shown by LDA score. (**E**) LefSe analysis results based on COG function prediction. The most significant function entries of the DSS (M) and DSS-MSC (T) groups were shown by LDA score. (**F**) The STAMP analysis results of KEGG function prediction. The most significant function entries of the DSS (M) and DSS-MSC (T) groups were analyzed by Welch's *t*-test. N: negative control group; M: DSS group; T: DSS-MSC group.

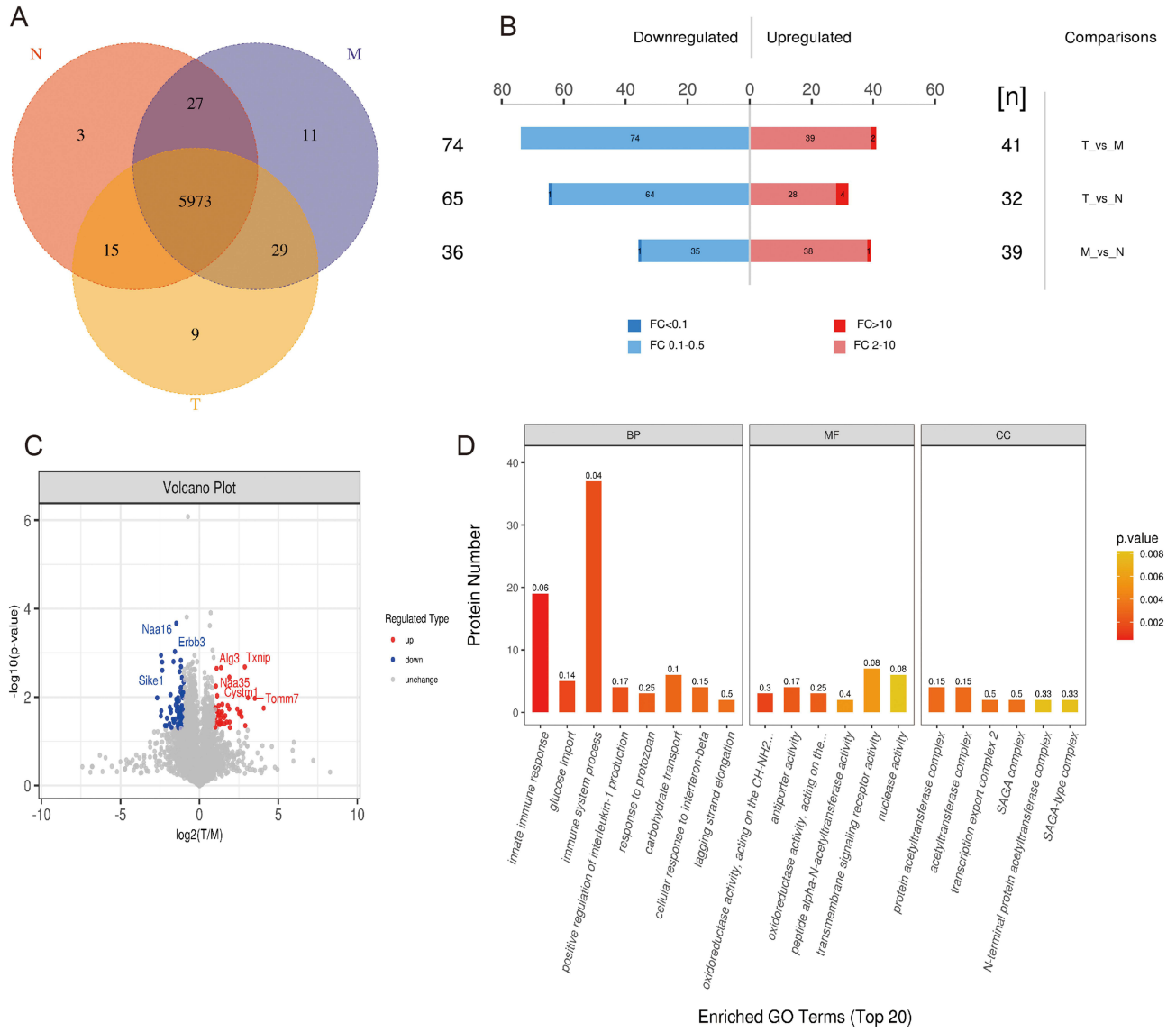

Figure 4 Label-free quantitative proteomics analysis of the significantly differential proteins between the DSS and MSC treatment groups. (**A**) The Venn diagram shows identified proteins between the sample groups. (**B**) The bar chart represents significantly expressed different proteins in each group (Fold change>2, P-value <0.05). (**C**) Volcano plot of differential proteins between the DSS and MSC treatment group. (**D**) Gene ontology (GO) analysis of biological process (BP), molecular function (MF) and cellular component (CC). The bar charts showed the number of proteins in each functional classification. The categories might be related to MSC therapeutic functions. MSC vs DSS group.

DSS-PBS group (Figure 7B), the H-score of MUC-1 intensity is shown on Figure S1C. *MUC-1* is involved in mechanism of action by MSCs in the treatment of IBD. The *MUC-1* inhibitor, GO-203, significantly inhibited the growth of the epithelial IEC-6 cells under different concentrations (Figure 7C). GO-203 inhibited the proliferation level of IEC-6 cells after treated for 48 h (Figure 7D). Through co-culture of IEC-6 cells and MSCs in the presence of GO-203, MSCs significantly increase IEC-6 cell viability after 48 h (Figure 7E). The schematic diagram of co-culture system is shown in Figure S1D.

Next, *MUC-1* was overexpressed in IEC-6 cells by lentivirus transfection, *MUC-1* protein level was verified by qRT-PCR and Western blot (Figures S1F and 7F). The infection efficiency of lentivirus was detected by flow cytometry (Figure S1G). *MUC-1* overexpression did not influence the proliferation level of IEC-6 cell both in 24 h and 48 h, whereas increased proliferation in 72 h (Figure 7G).

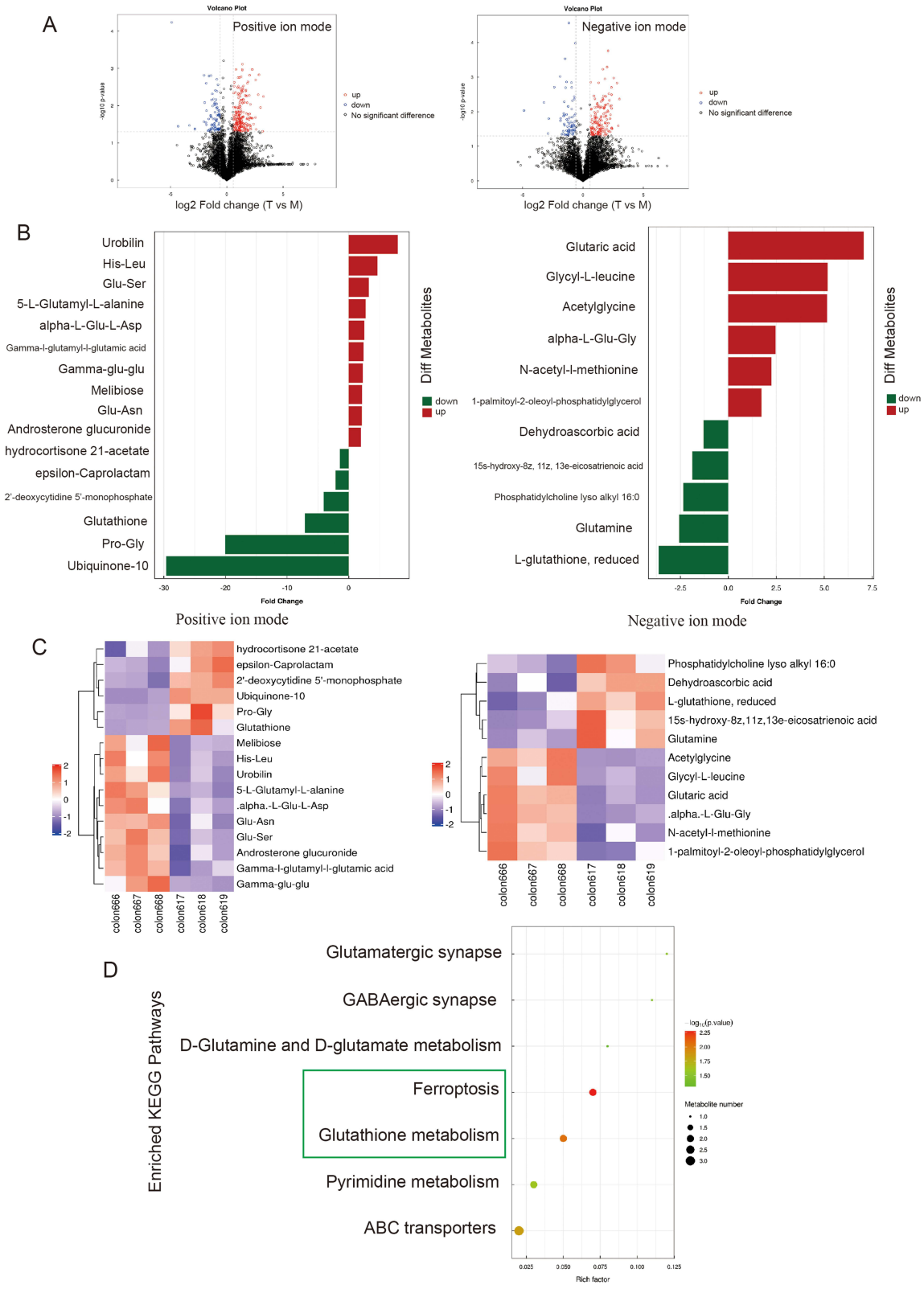

Figure 5 Untargeted metabolomics of DSS-induced colitis and MSC-treated colon tissues. (**A**) Volcano plot of the differential metabolites in the positive/negative ion modes. The red and blue dots represent the upregulated and downregulated metabolites in the MSC treatment group, respectively. (**B**) Significantly different metabolites in positive/negative ion mode (OPLS-DA VIP>1, P-value<0.05, MSC vs DSS group). The red and green bar graphs show upregulated and downregulated metabolites in the MSC treatment group, respectively. (**C**) Hierarchical clustering heatmap of significantly different metabolites in the positive/negative ion modes. Colons 666, 667, and 668 represent the MSC treatment group; Colons 617, 618, and 619 represent the DSS group. (**D**) KEGG enrichment analysis of metabolic pathways showing pathways that might be related to MSC therapeutic functions. The dot size reflects the number of metabolites enriched in the pathway, and the dot color represents the corresponding P value.

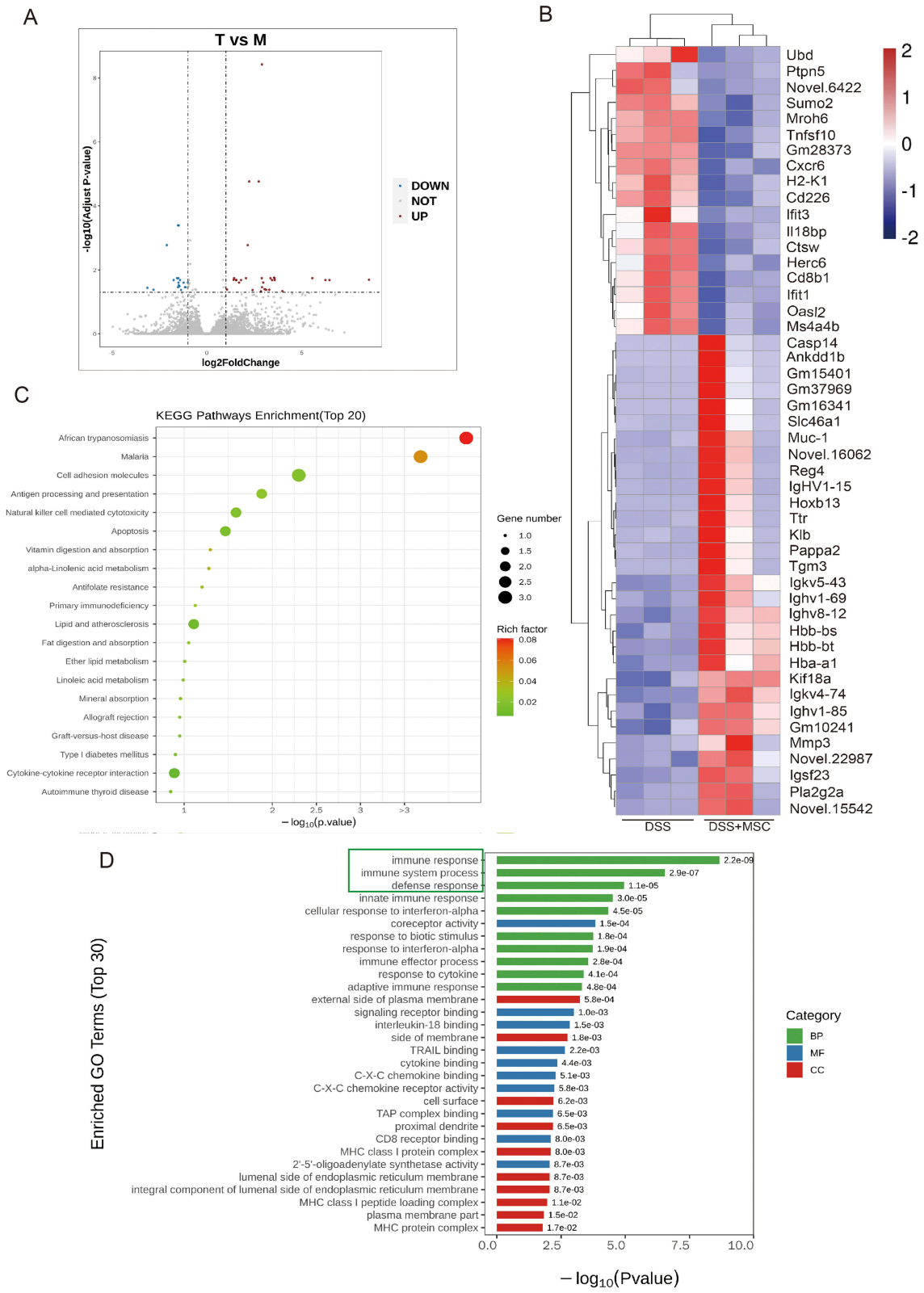

Figure 6 Transcriptome analysis of DSS-induced colitis and MSC treatment groups. (**A**) Volcano plot of differential genes between the DSS and MSC groups. (**B**) The heatmap of differential genes between DSS and MSC group (p-adj < 0.05, |log2foldchange| >1. (**C**) KEGG pathways enrichment analysis of differentially expressed genes. The dot size reflects the number of genes enriched in the pathway, and the color of the richness factor represents the number of differential genes in this pathway occupied with all the genes in this pathway. (**D**) Gene ontology (GO) entries of significant protein function categories encoded by the differential genes. The genetic properties are classified into the biological process (BP), molecular function (MF) and cellular component (CC). The categories shown are those that might be related to MSC therapeutic functions. -Log_{10} (P-value) was used to measure the expressions of differentially expressed genes.

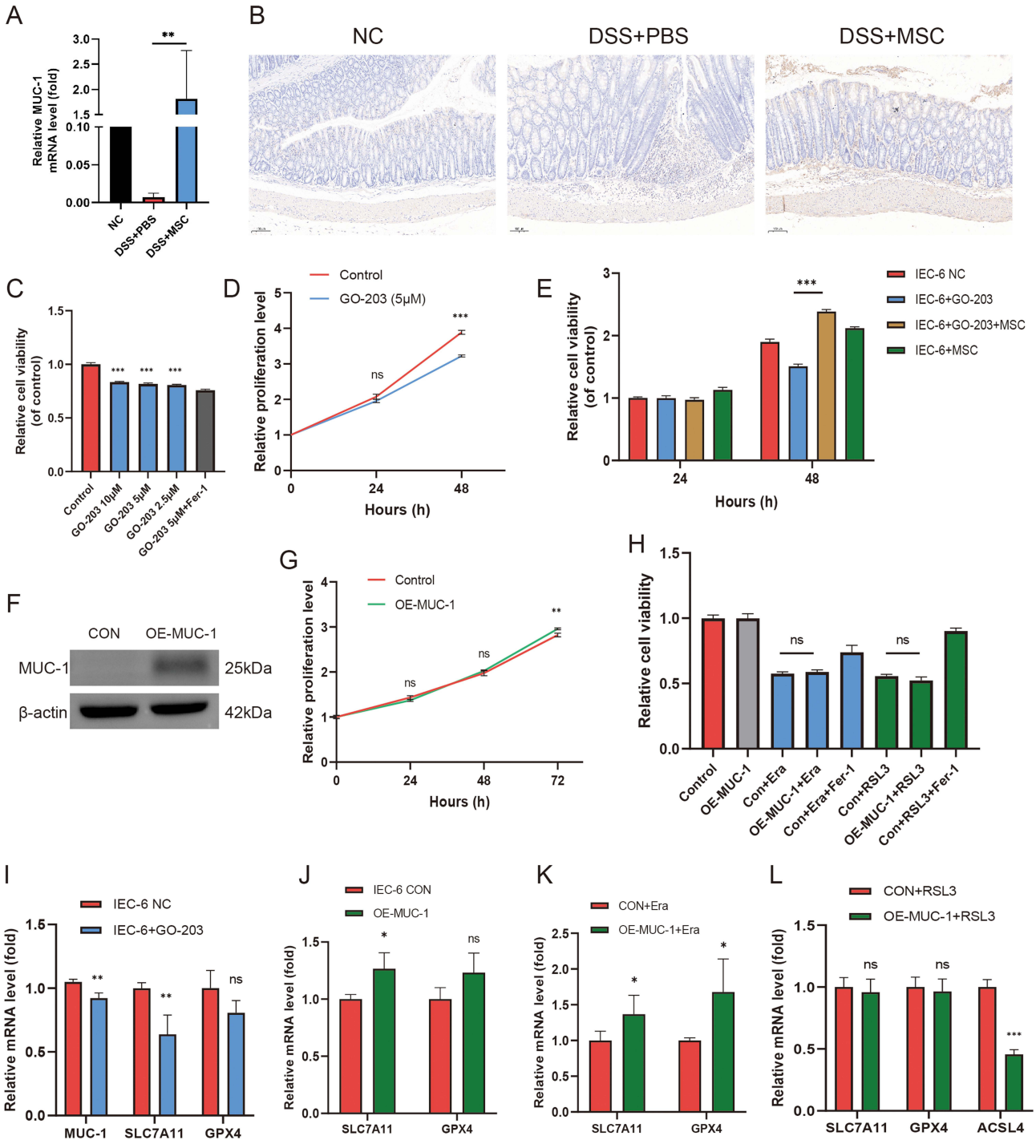

Figure 7 Ferroptosis-related genes play a role in DSS-induced colitis and MSCs reverse the process of ferroptosis. (**A**) The qPCR detection of *MUC-1* gene in colitis tissues. (**B**) The immunohistochemistry images of NC, DSS+PBS, and DSS+MSC groups in colon tissues (scale bar: 100μm). (**C**) The CCK-8 analysis of IEC-6 cell viability. The different concentration (10, 5, and 2.5μM) of GO-203 (MUC-1 inhibitor) was used to measure the cell viability at 48 h, GO-203 10, 5, and 2.5μM vs control. (**D**) The proliferation level of IEC-6 cells in the presence of GO-203 (5μM) at 24 h and 48 h measured by CCK-8 assay. (**E**) The cell viability of IEC-6 cells in the presence of GO-203 and co-culture with MSCs. (**F**) The Western blot analysis of MUC-1 expression after transfected with overexpressing MUC-1 lentivirus in IEC-6 cells. (**G**) The proliferation level of IEC-6 cells transfected with overexpressing MUC-1 lentivirus in 24 h, 48 h, and 72 h. (**H**) The IEC-6 cell viability after treated with erastin and RSL3 with the comparison of control and overexpressed MUC-1 group. (**I**) qRT-PCR analysis of *MUC-1, SLC7A11*, and *GPX4* after treated with GO-203 (5μM) for 48 h in IEC-6 cells. (**J**) qRT-PCR analysis of *SLC7A11* and *GPX4* after overexpressed *MUC-1* in IEC-6 cells. (**K**) qRT-PCR analysis of *SLC7A11* and *GPX4* in the presence of erastin in the control and overexpressed MUC-1 group. (**L**) qRT-PCR analysis of *SLC7A11, GPX4*, and *ACSL4* in the presence of RSL3 in the control and overexpressed MUC-1 group. Data are presented as mean ± SD. ***P < 0.001, **P < 0.01, *P < 0.05.

Abbreviation: ns, no significance.

The effects of *MUC-1* on ferroptosis of IEC-6 cells were further investigated. Treatment with erastin and RSL3 caused typical ferroptosis, which could be reversed by Fer-1, whereas *MUC-1* overexpression did not show a protective effect (Figure 7H). Treated with GO-203 caused down-regulation of *SLC7A11* and *GPX4* (Figure 7I). To detect whether overexpression of MUC-1 can regulate ferroptosis-related genes, *SLC7A11* and *GPX4* expression were detected by qRT-PCR, and the results showed that *SLC7A11* and *GPX4* were upregulated (Figure 7J). What's more, we investigated whether *MUC-1* could influence ferroptosis-related genes in the presence of erastin and RSL3, *MUC-1* overexpression increased expression of *SLC7A11* and *GPX4* after erastin treated (Figure 7K). While in RSL3-treated cells, *MUC-1* overexpression down-regulated *ACSL4* (Figure 7L). This indicates that *MUC-1* might be involved in the mechanism of action by MSCs in the treatment of IBD through inhibiting ferroptosis. Moreover, it might regulate the regeneration of the epithelial cell barrier in the DSS-MSC colitis model.

Discussion

IBD is caused by a dysregulated immune response combined with an intestinal epithelial barrier injury. MSCs can alleviate intestinal inflammation by regulating the immune response and enhancing intestinal healing. In this study, we extensively explored the mechanisms underlying the treatment of experimental colitis using human UC-MSCs by performing an integrative analysis of the transcriptome, proteomics, metabolomics, and gut microbiota in a mouse DSS-induced IBD model. DSS was used to induce colitis in mice because it disrupts intestinal barriers, disturbance of intestinal homeostasis, and extensive mucosal injury and inflammation. The DSS-induced experimental colitis is an ideal model to illustrate the therapeutic effect of MSC treatment.[20] In the present study, MSCs significantly ameliorated the severity of DSS-induced colitis by reducing the levels of pro-inflammation cytokines and restoring the lymphocyte subpopulation balance. Recent studies have indicated that microbial composition and intestinal metabolism are associated with IBD both in animal models and clinical therapy.[21,22] However, the effect of MSCs on the microbiota and metabolism is rarely reported. Using 16S genomic analysis, we revealed that MSC therapy changed the composition of microbiota by significantly increasing the abundance of *Firmicutes, Blautia, Roseburia, Helicobacter, and Lactobacillus*. Based on the findings, we suggest that MSCs can restore the gut microbiome and metabolism, leading to the recovery of the damaged mucosal barrier.

Lactobacillus accelerates intestinal stem cell regeneration to protect the integrity of intestinal mucosa through the activation of the STAT3 signaling pathway and secretion of IL-22.[23] *Lactobacillus* alleviates DSS-induced IBD by regulating oxidative stress and the immune response.[24] Moreover, *Lactobacillus* regulates the immune function by regulating Th17/Treg cell population in DSS-induced colitis in mice.[25] *Firmicutes* is a major phylum of gut commensals and can be decreased in various inflammatory disorders, including IBD.[26] The *Firmicutes/Bacteroidetes* (F/B) ratio is widely accepted to have an important influence in maintaining normal intestinal homeostasis.[27] In the present study, MSC therapy significantly increased the abundance of *Firmicutes* in IBD models, which may contribute to its therapeutic effects. Although the detailed mechanisms by which MSCs regulate the abundance of these probiotics remain unclear, the modulation of probiotics, such as *Firmicutes and Lactobacillus*, is the central to IBD recovery. This study demonstrated the MSC–gut bacteria interactions might play an important role in IBD therapy. Aberrant changes in immune cells, TGF-β, and gut microbiome and metabolites play important roles in DSS-induced IBD models.[28] MSC therapy could improve the recovery of immune responses and miRNA expression, restoration of the gut microbiota and production of metabolites.[29] Therefore, MSCs therapy changes the intestinal microbiota composition might affect the susceptibility to DSS colitis.

Recovery of the epithelial barrier is a major process in the treatment of IBD.[30] MSCs can protect the epithelial barrier against damage and enhance its healing by regulating epithelial cell proliferation and T cell immunity.[31] MSCs secret pleiotropic gut trophic factors and exosomes to suppress intestinal epithelial cell death, such as apoptosis and ferroptosis.[32,33] Apoptosis is involved in intestinal epithelial cell death in ulcerative colitis.[34] MSCs suppress the apoptosis of epithelial cell death and promote intestinal stem cell and epithelial regeneration. Ferroptosis is a form of regulated cell death characterized by the iron-dependent accumulation of lipid hydroperoxides to lethal levels.[35] Moreover, a new perspective on IBD pathogenesis suggests that ferroptosis is involved in inflammatory gut diseases.[36] In the present study, the proteomics and transcriptome profiles revealed that anti-inflammation and repair signals are involved in the effects of MSCs. Because oxidative stress is a mechanism underlying the pathophysiology of colitis, MSCs play an important role in preventing the disruption of antioxidant defenses in inflamed colon.[37] Sensitivity to ferroptosis is closely linked to the pathological process of IBD. Further studies have indicated that

ferroptosis inhibitor, ferrostatin-1 alleviates TNBS induced colitis.[38] In the present study, we identified that "immune pathways" might increase the gut signals related to cell death, such as ferroptosis and apoptosis. Transcriptome profiles revealed that the ferroptosis-related gene *MUC-1* is involved in the MSC therapy of IBD. *MUC-1* is a tumor-associated antigen that is down-regulated in IBD.[39] Previous reports have indicated that *MUC-1* might be a ferroptosis-related marker in ulcerative colitis[40] and might regulate cell ferroptosis.[41] Overexpression of *MUC-1*, together with loss of polarization and hypoxia are associated with apoptosis resistance.[42] *GPX4* is a ferroptosis inhibitor by utilizing reduced glutathione to convert lipid hydroperoxides to lipid alcohols.[43] System Xc^- contains subunits *SLC7A11* and *SLC3A2, GPX4* and *SLC7A11* inhibition cause accumulation of reactive oxygen species (ROS) and disruption of redox homeostasis.[44] In the present study, integrative analysis of ferroptosis-related genes revealed that *MUC-1* and *SLC7A11* are involved in IBD. *MUC-1* has an anti-inflammatory effect and reduced the level of oxidative stress through targeting TLR4/NF-κB signaling pathway,[45] and we demonstrated that UC-MSC protected the intestinal barrier function by significantly regulating *MUC-1* and ferroptosis regulators. Moreover, using the *MUC-1* inhibitor GO-203, we demonstrated that *MUC-1* was essential for intestinal epithelial cell growth and regeneration. Treated IEC-6 cells with GO-203 down-regulated ferroptosis-related genes, *SLC7A11* and *GPX4*. What's more, overexpression of *MUC-1* caused up-regulation of *SLC7A11* and *GPX4*, while down-regulation of *ACSL4* in ferroptotic state. Thus, upregulation of *MUC-1* plays an important role in MSC therapy and inhibition of ferroptosis.

Conclusions

MSCs ameliorated intestinal inflammation and modulated gut microbiota and metabolic disorders in DSS-induced colitis in mice. MSCs upregulated *MUC-1* to suppress cell death and enhance IBD recovery. This study reveals the underlying mechanisms of MSCs in the treatment of IBD and identifies potentially novel therapeutic avenues for IBD.

Abbreviations

CCK-8, Cell Counting Kit-8; COG, clusters of orthologous groups; DAI, Disease Activity Index; DSS: dextran sulphate sodium; GMP, Good Manufacturing Practice; GO, gene oncology; HE, hematoxylin and eosin; IBD, inflammatory bowel diseases; KEGG, Kyoto Encyclopedia of Genes and Genomes; LDA, linear discriminant analysis; LEfSe, linear discriminant analysis effect size; MSC, mesenchymal stem cell; NC, negative control; OPLS-DA, orthogonal partial least-squares discriminant analysis; PBS, phosphate-buffered saline; P_{adj}, adjust p value; qRT-PCR, quantitative real-time PCR; ROS, reactive oxygen species; SD, standard deviation; STAMP, statistical analysis of metagenomic profiles; UC, umbilical cord; VIP, variable importance projection.

Data Sharing Statement

The datasets generated and analyzed for this study are available from the corresponding author.

Ethics Approval

This study was conducted in accordance with the Declaration of Helsinki and approved by the Animal care and Use Committee of the Affiliated Hospital of Qingdao University, bearing approval number AHQU-MAL20210930.

Author Contributions

All authors made a significant contribution to the work reported, whether that is in the conception, study design, execution, acquisition of data, analysis and interpretation, or in all these areas; took part in drafting, revising or critically reviewing the article; gave final approval of the version to be published; have agreed on the journal to which the article has been submitted; and agree to be accountable for all aspects of the work.

Funding

This work was supported by the Natural Science Foundation of Shandong Province (ZR2020MH327) and National Key Research and Development Program (2017YFA0105303).

Disclosure

The authors have no conflicts of interest to declare.

References

1. Huldani H, Margiana R, Ahmad F, et al. Immunotherapy of inflammatory bowel disease (IBD) through mesenchymal stem cells. *Int Immunopharmacol*. 2022;107:108698. doi:10.1016/j.intimp.2022.108698
2. Fu X, Liu G, Halim A, Ju Y, Luo Q, Song AG. Mesenchymal stem cell migration and tissue repair. *Cells*. 2019;8(8):784. doi:10.3390/cells8080784
3. Panés J, García-Olmo D, Van Assche G, et al. Long-term efficacy and safety of stem cell therapy (Cx601) for complex perianal fistulas in patients with Crohn's disease. *Gastroenterology*. 2018;154(5):1334–1342.e4. doi:10.1053/j.gastro.2017.12.020
4. Lopez-Santalla M, Garin MI. Improving the efficacy of mesenchymal stem/stromal-based therapy for treatment of inflammatory bowel diseases. *Biomedicines*. 2021;9(11):1507. doi:10.3390/biomedicines9111507
5. Lightner A, Dadgar N, Matyas C, et al. A phase IB/IIA study of remestemcel-L, an allogeneic bone marrow-derived mesenchymal stem cell product, for the treatment of medically refractory ulcerative colitis: an interim analysis. *Colorectal Dis*. 2022;24(11):1358–1370. doi:10.1111/codi.16239
6. Li Y, Altemus J, Lightner AL. Mesenchymal stem cells and acellular products attenuate murine induced colitis. *Stem Cell Res Ther*. 2020;11(1):515. doi:10.1186/s13287-020-02025-7
7. Chen QQ, Yan L, Wang CZ, et al. Mesenchymal stem cells alleviate TNBS-induced colitis by modulating inflammatory and autoimmune responses. *World J Gastroenterol*. 2013;19(29):4702–4717. doi:10.3748/wjg.v19.i29.4702
8. Wang G, Joel MDM, Yuan J, et al. Human umbilical cord mesenchymal stem cells alleviate inflammatory bowel disease by inhibiting ERK phosphorylation in neutrophils. *Inflammopharmacology*. 2020;28(2):603–616. doi:10.1007/s10787-019-00683-5
9. Yang S, Liang X, Song J, et al. A novel therapeutic approach for inflammatory bowel disease by exosomes derived from human umbilical cord mesenchymal stem cells to repair intestinal barrier via TSG-6. *Stem Cell Res Ther*. 2021;12(1):315. doi:10.1186/s13287-021-02404-8
10. Cai X, Zhang ZY, Yuan JT, et al. hucMSC-derived exosomes attenuate colitis by regulating macrophage pyroptosis via the miR-378a-5p/NLRP3 axis. *Stem Cell Res Ther*. 2021;12(1):416. doi:10.1186/s13287-021-02492-6
11. Qi L, Wu J, Zhu S, et al. Mesenchymal stem cells alleviate inflammatory bowel disease via Tr1 cells. *Stem Cell Reviews Rep*. 2022;18(7):2444–2457. doi:10.1007/s12015-022-10353-9
12. Xu J, Wang X, Chen J, et al. Embryonic stem cell-derived mesenchymal stem cells promote colon epithelial integrity and regeneration by elevating circulating IGF-1 in colitis mice. *Theranostics*. 2020;10(26):12204–12222. doi:10.7150/thno.47683
13. Soontararak S, Chow L, Johnson V, et al. Mesenchymal stem cells (MSC) derived from induced pluripotent stem cells (iPSC) equivalent to adipose-derived msc in promoting intestinal healing and microbiome normalization in mouse inflammatory bowel disease model. *Stem Cells Transl Med*. 2018;7(6):456–467. doi:10.1002/sctm.17-0305
14. Gu L, Ren F, Fang X, Yuan L, Liu G, Wang S. Exosomal microRNA-181a derived from mesenchymal stem cells improves gut microbiota composition, barrier function, and inflammatory status in an experimental colitis model. *Front Med*. 2021;8:660614. doi:10.3389/fmed.2021.660614
15. Wirtz S, Popp V, Kindermann M, et al. Chemically induced mouse models of acute and chronic intestinal inflammation. *Nat Protoc*. 2017;12(7):1295–1309. doi:10.1038/nprot.2017.044
16. Liu P, Lin C, Liu Z, et al. Inhibition of ALG3 stimulates cancer cell immunogenic ferroptosis to potentiate immunotherapy. *Cellular Mol Life Sci*. 2022;79(7):352. doi:10.1007/s00018-022-04365-4
17. Szpigel A, Hainault I, Carlier A, et al. Lipid environment induces ER stress, TXNIP expression and inflammation in immune cells of individuals with type 2 diabetes. *Diabetologia*. 2018;61(2):399–412. doi:10.1007/s00125-017-4462-5
18. Shi D, Qi M, Zhou L, et al. Endothelial mitochondrial preprotein translocase Tomm7-Rac1 signaling axis dominates cerebrovascular network homeostasis. *Arterioscler Thromb Vasc Biol*. 2018;38(11):2665–2677. doi:10.1161/atvbaha.118.311538
19. Tian H, Ding M, Guo Y, et al. Use of transcriptomic analysis to identify microRNAs related to the effect of stress on thymus immune function in a chicken stress model. *Res Vet Sci*. 2021;140:233–241. doi:10.1016/j.rvsc.2021.09.004
20. Gonzalez-Rey E, Anderson P, González M, Rico L, Büscher D, Delgado M. Human adult stem cells derived from adipose tissue protect against experimental colitis and sepsis. *Gut*. 2009;58(7):929–939. doi:10.1136/gut.2008.168534
21. Nishida A, Inoue R, Inatomi O, Bamba S, Naito Y, Andoh A. Gut microbiota in the pathogenesis of inflammatory bowel disease. *Clin J Gastroenterol*. 2018;11(1):1–10. doi:10.1007/s12328-017-0813-5
22. Lavelle A, Sokol H. Gut microbiota-derived metabolites as key actors in inflammatory bowel disease. *Nat Rev Gastroenterol Hepatol*. 2020;17(4):223–237. doi:10.1038/s41575-019-0258-z
23. Hou Q, Ye L, Liu H, et al. Lactobacillus accelerates ISCs regeneration to protect the integrity of intestinal mucosa through activation of STAT3 signaling pathway induced by LPLs secretion of IL-22. *Cell Death Differ*. 2018;25(9):1657–1670. doi:10.1038/s41418-018-0070-2
24. Pan Y, Ning Y, Hu J, Wang Z, Chen X, Zhao X. The preventive effect of Lactobacillus plantarum ZS62 on DSS-induced ibd by regulating oxidative stress and the immune response. *Oxid Med Cell Longev*. 2021;2021:9416794. doi:10.1155/2021/9416794
25. Huang J, Yang Z, Li Y, et al. Lactobacillus paracasei R3 protects against dextran sulfate sodium (DSS)-induced colitis in mice via regulating Th17/Treg cell balance. *J Transl Med*. 2021;19(1):356. doi:10.1186/s12967-021-02943-x
26. Gill T, Asquith M, Rosenbaum JT, Colbert RA. The intestinal microbiome in spondyloarthritis. *Curr Opin Rheumatol*. 2015;27(4):319–325. doi:10.1097/bor.0000000000000187
27. Stojanov S, Berlec A, Štrukelj B. The influence of probiotics on the Firmicutes/Bacteroidetes ratio in the treatment of obesity and inflammatory bowel disease. *Microorganisms*. 2020;8(11):Nov. doi:10.3390/microorganisms8111715
28. Wang Y, Huang B, Jin T, Ocansey DKW, Jiang J, Mao F. Intestinal fibrosis in inflammatory bowel disease and the prospects of mesenchymal stem cell therapy. *Front Immunol*. 2022;13:835005. doi:10.3389/fimmu.2022.835005
29. Kim WK, Han DH, Jang YJ, et al. Alleviation of DSS-induced colitis via Lactobacillus acidophilus treatment in mice. *Food Funct*. 2021;12(1):340–350. doi:10.1039/d0fo01724h

30. Parikh K, Antanaviciute A, Fawkner-Corbett D, et al. Colonic epithelial cell diversity in health and inflammatory bowel disease. *Nature*. 2019;567(7746):49–55. doi:10.1038/s41586-019-0992-y
31. Gao JG, Yu MS, Zhang MM, et al. Adipose-derived mesenchymal stem cells alleviate TNBS-induced colitis in rats by influencing intestinal epithelial cell regeneration, Wnt signaling, and T cell immunity. *World J Gastroenterol*. 2020;26(26):3750–3766. doi:10.3748/wjg.v26.i26.3750
32. Watanabe S, Arimura Y, Nagaishi K, et al. Conditioned mesenchymal stem cells produce pleiotropic gut trophic factors. *J Gastroenterol*. 2014;49(2):270–282. doi:10.1007/s00535-013-0901-3
33. Harrell CR, Jovicic N, Djonov V, Arsenijevic N, Volarevic V. Mesenchymal stem cell-derived exosomes and other extracellular vesicles as new remedies in the therapy of inflammatory diseases. *Cells*. 2019;8(12):1605. doi:10.3390/cells8121605
34. Xu M, Tao J, Yang Y, et al. Ferroptosis involves in intestinal epithelial cell death in ulcerative colitis. *Cell Death Dis*. 2020;11(2):86. doi:10.1038/s41419-020-2299-1
35. Chen X, Kang R, Kroemer G, Tang D. Ferroptosis in infection, inflammation, and immunity. *J Exp Med*. 2021;218(6). doi:10.1084/jem.20210518
36. Xu S, He Y, Lin L, Chen P, Chen M, Zhang S. The emerging role of ferroptosis in intestinal disease. *Cell Death Dis*. 2021;12(4):289. doi:10.1038/s41419-021-03559-1
37. da Costa Gonçalves F, Grings M, Nunes NS, et al. Antioxidant properties of mesenchymal stem cells against oxidative stress in a murine model of colitis. *Biotechnol Lett*. 2017;39(4):613–622. doi:10.1007/s10529-016-2272-3
38. Xu J, Liu S, Cui Z, et al. Ferrostatin-1 alleviated TNBS induced colitis via the inhibition of ferroptosis. *Biochem Biophys Res Commun*. 2021;573:48–54. doi:10.1016/j.bbrc.2021.08.018
39. Poh TW, Madsen CS, Gorman JE, et al. Downregulation of hematopoietic MUC1 during experimental colitis increases tumor-promoting myeloid-derived suppressor cells. *Clin Cancer Res*. 2013;19(18):5039–5052. doi:10.1158/1078-0432.Ccr-13-0278
40. Cui DJ, Chen C, Yuan WQ, Yang YH, Han L. Integrative analysis of ferroptosis-related genes in ulcerative colitis. *J Int Med Res*. 2021;49(9):3000605211042975. doi:10.1177/03000605211042975
41. Wang YM, Gong FC, Qi X, et al. Mucin 1 inhibits ferroptosis and sensitizes vitamin E to alleviate sepsis-induced acute lung injury through GSK3β/Keap1-Nrf2-GPX4 pathway. *Oxid Med Cell Longev*. 2022;2022:2405943. doi:10.1155/2022/2405943
42. Supruniuk K, Radziejewska I. MUC1 is an oncoprotein with a significant role in apoptosis (Review). *Int J Oncol*. 2021;59(3). doi:10.3892/ijo.2021.5248
43. Forcina G, Dixon S. GPX4 at the crossroads of lipid homeostasis and ferroptosis. *Proteomics*. 2019;19(18):e1800311. doi:10.1002/pmic.201800311
44. Chen X, Li J, Kang R, Klionsky D, Tang D. Ferroptosis: machinery and regulation. *Autophagy*. 2021;17(9):2054–2081. doi:10.1080/15548627.2020.1810918
45. Ye C, Xu B, Yang J, et al. Mucin1 relieves acute lung injury by inhibiting inflammation and oxidative stress. *Eur J Histochemistry*. 2021;65(4):56. doi:10.4081/ejh.2021.3331

Journal of Inflammation Research Dovepress

Publish your work in this journal

The Journal of Inflammation Research is an international, peer-reviewed open-access journal that welcomes laboratory and clinical findings on the molecular basis, cell biology and pharmacology of inflammation including original research, reviews, symposium reports, hypothesis formation and commentaries on: acute/chronic inflammation; mediators of inflammation; cellular processes; molecular mechanisms; pharmacology and novel anti-inflammatory drugs; clinical conditions involving inflammation. The manuscript management system is completely online and includes a very quick and fair peer-review system. Visit http://www.dovepress.com/testimonials.php to read real quotes from published authors.

Submit your manuscript here: https://www.dovepress.com/journal-of-inflammation-research-journal